International Journal of Civil Engineering and Technology (IJCIET)
Volume 10, Issue 2, February 2019, pp.2227–2239, Article ID: IJCIET_10_02_221
Available online at http://www.iaeme.com/ijciet/issues.asp?JType=IJCIET&VType=10&IType=2
ISSN Print: 0976-6308 and ISSN Online: 0976-6316

STM EXPERIMENTAL VERIFICATION FOR REINFORCED CONCRETE CONTINUOUS DEEP BEAMS

Taha K. Mohammedali
University of Diyala, Diyala, Iraq

Ali Mustafa Jalil
M.Sc. Student, University of Diyala, Civil Engineering, Diyala, Iraq

Khattab Saleem Abdul-Razzaq
Prof. Dr., University of Diyala, Civil Engineering, Diyala, Iraq

Abbas H. Mohammed
Dr., University of Diyala, Civil Engineering, Diyala, Iraq

ABSTRACT

Strut-and-tie modelling (STM) is a very useful tool to analyze and design the irregular concrete deep members. This work presents the results of the experimental tests conducted on two reinforced concrete continuous deep beams that had a constant cross section of 140 mm×500 mm and a total length of 1700 mm. The beams are subjected to single and uniformly distributed load. Each test specimen is designed by using the STM that presented in Appendix A of ACI 318-14 provisions. The cracking load, failure load, deflection, crack pattern, steel reinforcement strains, concrete surface average strains and locations of failure for the tested beams were observed, recorded and discussed. The experimental results (P_f) and (W_f) are compared with the STM theoretical results (P_{STM}). Test results indicated that each beam carried loads greater than the STM theoretical design load. In other words, results show that the STM is a conservative method that gives the designers wide flexibility. More specifically, in this study, in case of singly concentrated force, P_{STM} is less than P_f by about 21%, while P_{STM} is less than W_f by about 27% in case of uniformly distributed load.

Keywords: Strut and Tie, Experimental verification, Reinforced concrete, Continuous deep beams.

Cite this Article: Taha K. Mohammedali, Ali Mustafa Jalil, Khattab Saleem Abdul-Razzaq and Abbas H. Mohammed, STM Experimental Verification For Reinforced Concrete Continuous Deep Beams, International Journal of Civil Engineering and Technology (IJCIET), 10 (2), 2019, pp. 2227–2239.
http://www.iaeme.com/ijciet/issues.asp?JType=IJCIET&VType=10&IType=2

1. INTRODUCTION

With the rapid development of construction in many countries, continuous deep beam at its behavior predication is a subject of attention where received wide interest from researchers [1-7]. The ACI 318M-14 Code defines deep beams as [8]: Members subjected to loads on one face and supported on the reverse face so that compressive struts can grow between the loading and supporting points. Beams classified as deep when 1 or 2 have: 1) Clear spans $l_n \leq$ 4h, where h is the whole depth of the member; or 2) Zones of the concentrated loadings within 2h from the support face.

The critical section of shear must be taken into account at a distance from support face at about 0.15 $ln \leq$ d for deep beams that loaded uniformly and about 0.5 a $\leq$ d for deep beams that loaded with concentrated forces, where (a) is the distance from center of support to concentrated load or shear span, and (d) is distance from extreme compressive fiber to the tension reinforcement centroid [9].

In the design of concrete structures, there are many limitations in the use of classical beam theory and classical sectional analysis. In areas where there is a change in loading or cross section, these typical design techniques often do not produce significant results. These regions are often called D-regions or disturbed regions [9]. STM can be used to analyze these D-regions. In theory, STM provides lower-bound and safe designs [10-15]. Strut-and-tie modeling is a very useful tool to design the unusual or complex reinforced concrete members. It is a fact that there is important literature on strut-and-tie modeling, but there are not a large number of experimental validations of using it in reinforced concrete deep beams. Therefore, this study is considered here as an attempt to investigate the application of this theory experimentally.

2. EXPERIMENTAL PROGRAM

The experimental program consists of constructing and testing two reinforced concrete continuous deep beams. The beams DBC and DBU had the same lengths as shown in Figure 1. They have a length of 1700 mm, a height of 500 mm and a width of 140 mm. The beams are designed to fail in shear. The amount of flexural bottom reinforcement is 4ϕ16mm, i.e. ρ = 0.0129, where ρ is the top and bottom reinforcement ratio for flexure. The shear reinforcement amount for the beams is ϕ4mm@70mm. The beams DBC and DBU are tested with a clear span (l_n) of 600 mm which results in a ratio of clear span (l_n) to overall depth (h) equals to l_n/h=1.2 which is less than 4 [8]. To recognize beams designation simply, Table 1 shows the system followed in beams designation.

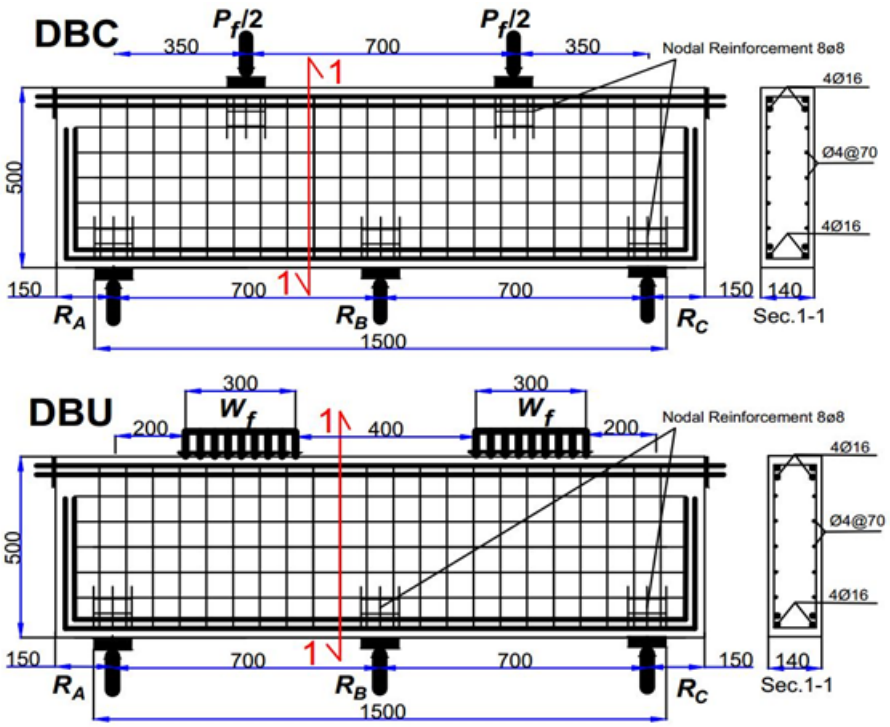

Figure 1 Reinforcement details of specimens, all dimensions in mm

Table 1 Beams designation way

Letter	Meaning
DB	Continuous Deep Beam
C	Subjected to Concentrated Force (P_f)
U	Subjected to Uniformly Distributed load (W_f)

2.1. Material properties of concrete beams

Ordinary Portland cement type I of Tasluja factory is used. Al-Duze graded natural sand with a specific gravity of 2.6 is used. 10 mm maximum particles size of crushed gravel is used in mixtures. Deformed steel bars of 16 mm were used as bottom and top reinforcement for the beams DBC and DBU which are, specifically, 4ϕ16. Deformed steel bars of diameter 4 mm are used for the vertical and horizontal shear reinforcement of the beams, specifically, ϕ4@70mm. Table 2 shows the mechanical properties of used steel. Test results indicate that the adopted steel reinforcement as longitudinal bars and shear reinforcement stirrups conform to the requirements of ASTM A615/A615M-05 [16] and ASTMA496-02 [17], respectively.

Table 2 Mechanical properties of reinforcing steel bars*

Type of used bars	Nominal bar diameter (mm)	Measured bar diameter (mm)	Yield stress (MPa)	Ultimate stress (MPa)
Flexural reinforcement	16	15.98	480	725
Shear web reinforcement	4	4.02	600	810

*Steel bars are tested by using the testing machine Jet materials Ltd. Company that has 500 kN capacity available at the Laboratory of Structural Engineering at the College of Engineering \ University of Diyala.

Through casting the beams, six cylinders of 150 x 300mm are cast. Three cylinders are used to measure the splitting tensile strength (f_{ct}) and the remaining three are used to measure concrete compressive strength (f'_c). Besides, for testing the concrete modulus of rapture (f_r), three 500mm x 100mm x100mm prisms are tested. About 24 hours after casting, all beams are demolded, and then cured by continuous covering by moist thick canvas for 28 days. Then, the beams are white painted to assist in the test crack observation. The mix proportions of materials used in this study are summarized in Table 3, while the properties of the mixed concrete are presented in Table 4.

Table 3 Mix proportions of concrete

Mix no.	Cement content (kg/m^3)	Sand content (kg/m^3)	Gravel content (kg/m^3)	Water (kg/m^3)	Water/ Cement ratio (w/c)	Cylinder compressive strength, $f'c$ MPa (28 days)
1	420	750	780	250	0.595	29.55
2*	400	750	780	240	0.600	24.95
3	400	750	780	250	0.625	22.54

*This mix is used to cast all specimens.

Table 4 Mix proportions of the used concrete

Beam	f'_c (MPa)	f_{ct} (MPa)	f_r (MPa)	$E_c{}^*$ (MPa)
DBC	26.94	3.08	4.22	24395
DBC	26.40	3.19	4.25	24149

*The values of E_c are derived from ($4700\sqrt{f'_c}$) provided by (ACI 318M-2014

2.2. Test set-up and instrumentation

The deep beams are tested using a hydraulically universal testing machine type 8551 M.F.L.L that has a capacity of 3000 kN. The tests are implemented using monotonic static loading till failure at the Structural Laboratory / College of Engineering / Al-Mustansiriya University. Two dial gauges of 0.01 mm accuracy are fixed under the centers of spans to calculate mid-span deflection. Strain gauges are prepared and fixed on each tested beam to calculate strains in steel bars and concrete. The strain gauges used in the experimental program are wire-type BFH120-3AA-X3 of the size 25 x 2.3 mm for concrete and 6 x 2.3 mm for steel reinforcement with a resistance of 120 Ω.

3. EXPERIMENTAL RESULTS

All beams are tested under incremental static load up to failure. The results are analyzed and compared in different stages of loading. The load-deflection curves are plotted. The first cracking and failure loads are recorded. The crack propagation, crack patterns and type of cracks, steel reinforcement strains, concrete surface average strains are marked and classified after each load increment.

3.1. General behavior of beams

Table 5 shows summary of the experimental test results for beams. It is seen that the beams DBC and DBU carried more than the STM theoretical design loads. A comparison between the experimental ultimate loads and STM results for DBC and DBU is shown in Figure 2 in which it is clear that the differences are 20.7% and 27.38% for DBC and DBU, respectively. Figure 3, 4 and 5 show flexural, diagonal cracking and experimental loads for beams. It is seen that the positive flexural cracks took place at about 22% and 39% of the ultimate loads for DBC and DBU, respectively. From the other hand, the diagonal cracks took place at about 26% and 45% of the ultimate loads, while the negative flexural cracks took place at about 33% and 30% of the ultimate loads for DBC and DBU, respectively. The general behavior of the tested beams can be described as follows:

Table 5 Summary of test results for tested beams

Specimens	P_{STM} (kN)	$P_{p.crack}$ (kN)	$P_{diag.crack}$ (kN)	$P_{n.crack}$ (kN)	P_f (kN)	P_f/P_{STM}	$P_{p.crack}/P_f$ (%)	$P_{diag.crack}/P_f$ (%)	$P_{n.crack}/P_f$ (%)	$\Delta_{p.crack}$ (mm)	$\Delta_{diag.crack}$ (mm)	$\Delta_{n.crack}$ (mm)	Δ_f (mm)
DBC	816.3	225	310	340	1030	1.26	21.84	30.1	33.01	1.41	1.87	2.11	6.85
DBU	1034.8	550	600	475	1425	1.38	38.6	42.1	33.33	1.02	1.13	0.87	3.4

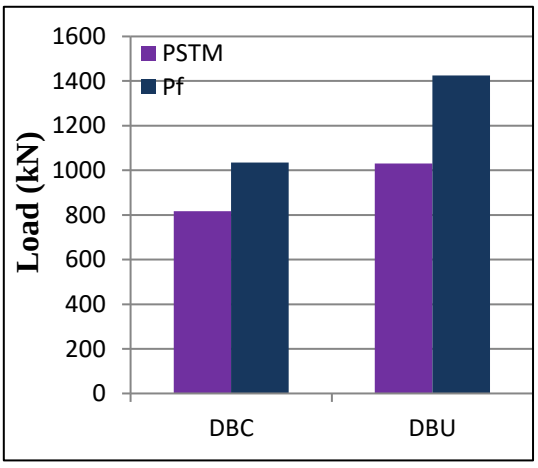

Figure 2 The STM and the experimental ultimate loads for beams

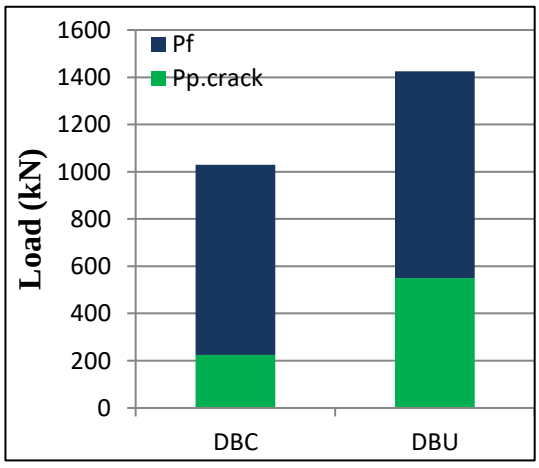

Figure 3 Positive flexural cracking and experimental ultimate loads for beams

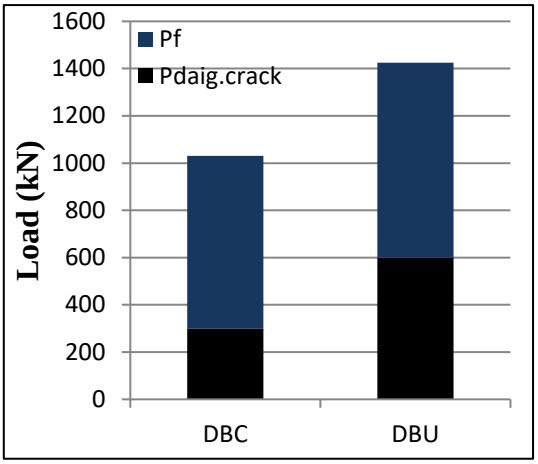

Figure 4 Diagonal cracking and experimental ultimate loads for beams

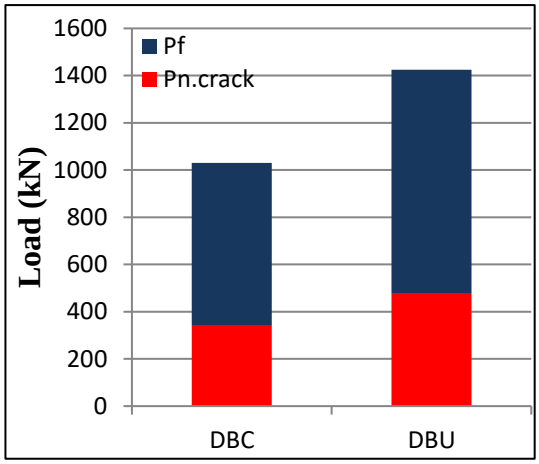

Figure 5 Negative flexural cracking and experimental ultimate loads for beams

*3.*1*.1 The specimen DBC*

The first visible flexural cracks are observed at 22% of the ultimate load in the positive bending moment regions as shown in Figure 7. These flexural cracks continued propagating upward in the load point direction. After that, first shear cracks were started at about 26% of the ultimate load near the nodal zones of support. The first flexural cracks over the middle support occurred at about 33% of the ultimate load. With more loading, major diagonal cracks extended to join the applied load and the supports. About failure, the diagonal cracks became wider. Finally, the failure took place by additional widening of the main inclined shear cracks between the left external support and the applied load, i.e. ***diagonal splitting failure in the left external strut.***

Figure 7 DBC specimen after test

3.1.2 The specimen (DBU): The first seen flexural cracks showed up at about 30% of the ultimate load in the negative bending moment region. At about 39% of the ultimate load, the first flexural cracks showed up in the positive bending moment region as shown in Figure 8. Then, at about 45% of the ultimate load, the first inclined shear cracks showed up in the right internal shear span. After that, more flexural and diagonal cracks developed and major diagonal cracks extended to join the applied loads and the internal support. Finally, the specimen failed in ***diagonal splitting failure at the right internal strut.***

Figure 8 DBU specimen after test

3.2. Load-deflection behavior

The mid-span deflection curves for the tested beams as a function of the total applied loads are shown in Figure 9 and 10. They are essential for describing the behavior of a beam at various stages of loading. Those mid-span deflection curves are those recorded at the failed span. In both specimens, the load-deflection curves were approximately linear in the main parts of the loading and after that the curves began to bend to some extent. This shows that shear behavior is the dominant behavior which causes brittle failure. The brittle failure decreased the specimen ductility and decreased the structural element strength below the flexural capacity.

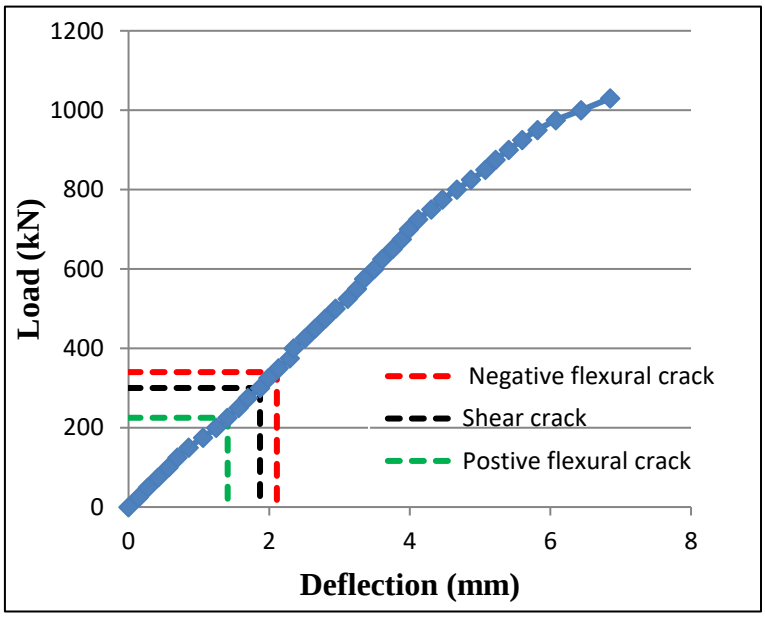

Figure 9 Load-midspan deflection for CDB

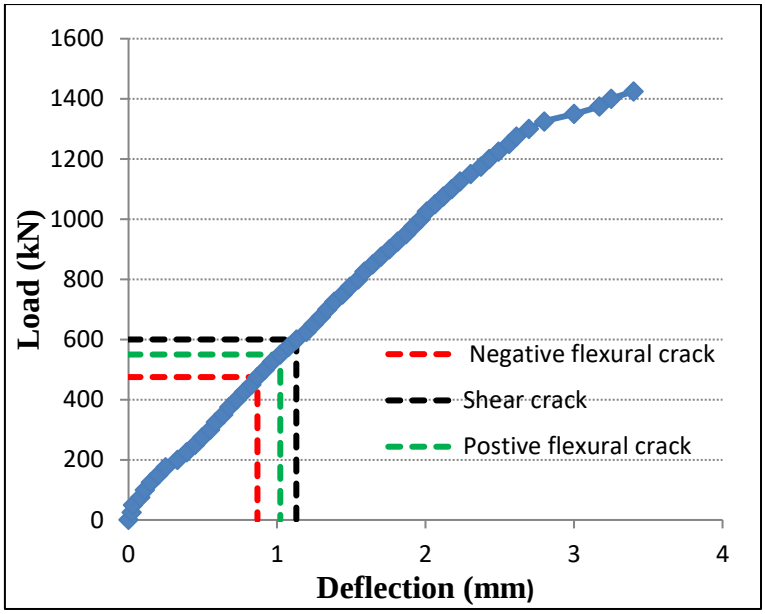

Figure 10 Load-midspan deflection for UDB

3.3. Average concrete surface strains

On front side of the tested beams, at struts and ties, concrete strains were measured. The surface strain values in concrete are investigated in the locations of inclined struts (in the middle of the lines joining the load and the support points) in addition to the horizontal struts as shown in Figure 11 and 12. The concrete surface strains gave an idea regarding the maximum concrete compressive surface strains and showed the development of the first crack of shear. Moreover, concrete strain gauges assisted to comprehend the forces flow from the loading to the near supporting points.

At the beginning of loading, both beams showed linear behavior and the propagated strains of concrete surface were minor. More loading led to an abrupt change in the average strain values where the formation of first shear crack took place, more specifically, at 26% and 45% of the ultimate loads for DBC and DBU, respectively. Then cracking in concrete turn out to be visible and strain values increased rapidly according to the applied load. Inclined strut gauges were affected by cracks through readings that increased after the appearance of the first diagonal cracks. It was seen that at failure, the maximum compressive strain took place in inclined struts at about 0.0022. Moreover, the maximum compressive strain occurred in horizontal struts at about 0.0018.

Based on strain diagrams shown in Figure 11 and Fig. 12, the load which made a first abrupt increase in the strain values means the first shear crack formation load. The estimated first shear cracking strain from the visually observed and the diagrams are listed in Table 6. It is seen that the differences between the both readings are small. That took place due to the fact that strain gauges can predict cracking more accurate than visual inspection.

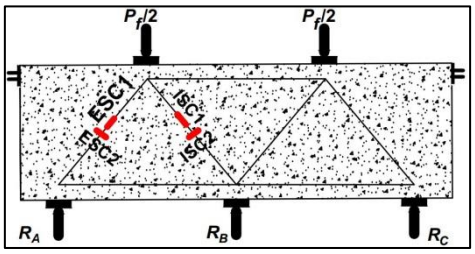

Strain gauge location

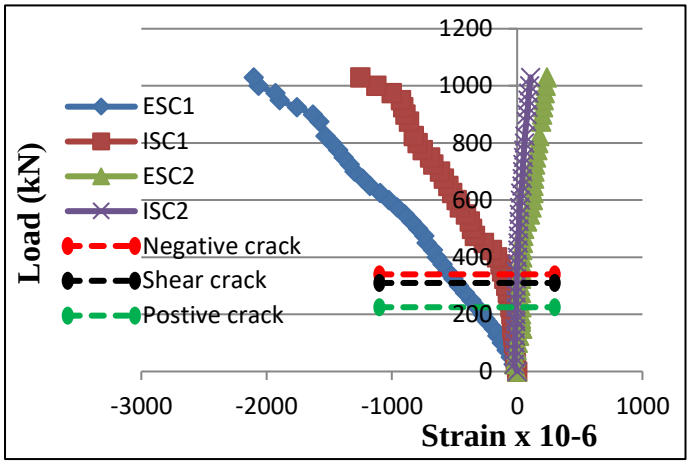

Figure 11 Applied load versus average concrete compressive surface strains for beam DBC

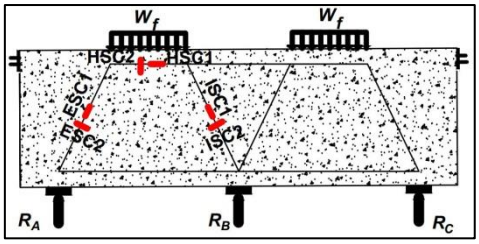

Strain gauge location

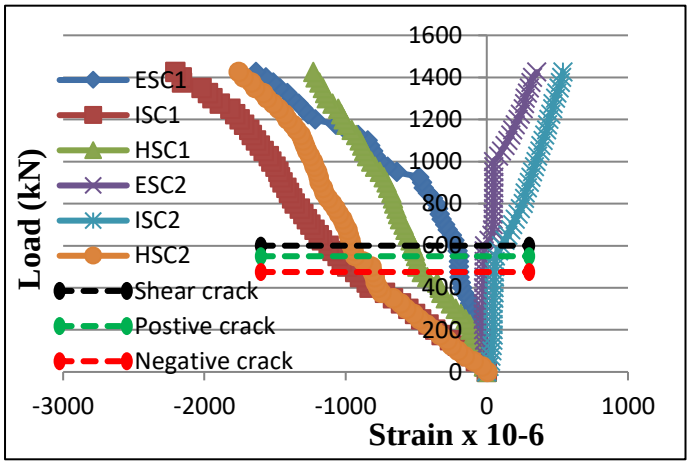

Figure 12 Applied load versus average concrete compressive surface strains for beam DBU

3.4. Steel reinforcement strain

Table 6 Values of experimental cracking loads and the cracking loads that obtained from strain diagrams

Specimens	P_f (kN)	Visual readings		Strain gauge readings	
		1st visual shear cracking load (kN)	% 1st shear cracking load / failure load	Estimated 1st shear cracking load from strain diagram (kN)	% 1st shear cracking load / failure load
DBC	1030	340	33.01	300	29.13
DBU	1425	630	44.21	600	42.11

The strain values are investigated in the locations of main longitudinal top and bottom reinforcement bars as shown in Figure 13 and 14. In addition to that, inclined ϕ4mm bars are added in order to determine the strain that takes place in concrete at the inclined struts.

According to the results of testing steel bars presented in Table 3, the yield strain of the bar ϕ4mm is ε_{yield} =3000 με and the yield strain of the bar ϕ16mm is ε_{yield} =2400 με. For all gauges, the strain values are recorded at different stages of loading until the failure. After the development of the crack, sudden changes in the steel strain readings are logged.

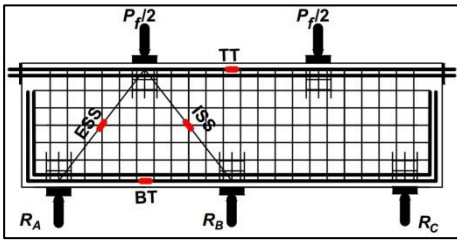

Strain gauge location

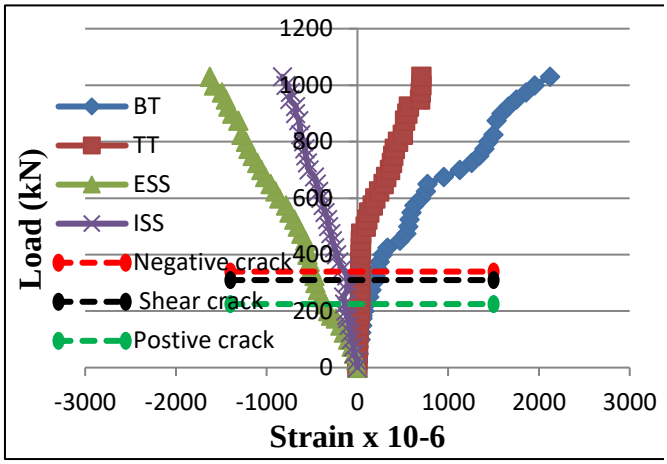

Figure 13 Applied load versus steel strain for beam DBC

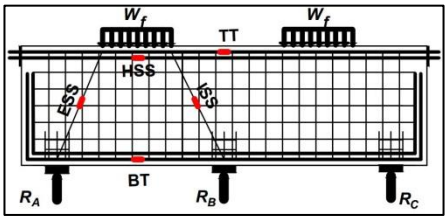

Strain gauge location

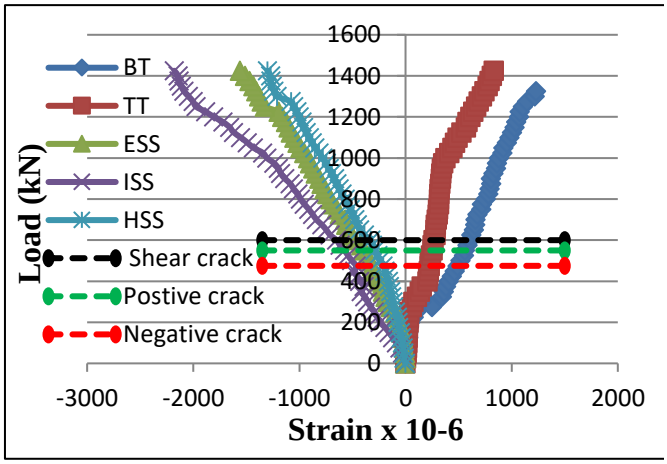

Figure 14 Applied load versus steel strain for beam DBU

4. CONCLUSIONS

Based on test results, the following conclusions can be drawn:

1. In shear strength predicting of deep beams, Strut-and-Tie Model (STM) of Appendix A, in ACI 318-14 is conservative and shows lower-bound design in comparison with the laboratory work**.** STM predicts continuous deep beam strength that was tested under two types of loading; uniformly distributed load and 2-concentrated forces are lesser than laboratory strengths by about 21% and 27.4%, respectively.

2. The curves of load-deflection are approximately linear in the major loading portion and then the curves began to bend to some extent. Therefore, it could be concluded that the shear deformation is the predominant behavior which leads to brittle failure. This brittle failure noticeably reduces the ductility and reduces the flexural capacity of the continuous reinforced concrete beams.
3. The first positive flexural cracks occur at around 22% and 39% of the failure load in the deep beams that subjected to concentrated forces and uniformly distributed load, respectively. The first diagonal cracks occur at around 26% and 45% of the failure load, respectively. From the other hand, the first negative flexural cracks occur at around 33% and 30% of the failure load, respectively.
4. The first visible shear cracking load and the estimated first shear cracking load from strain diagram are relatively close. That took place due to the fact that strain gauges can predict cracking more accurate than visual inspection.
5. The compressive strain behavior for deep beams that were tested under uniformly distributed load and 2-concentrated forces is almost similar. It is seen that at failure, the maximum compressive strain in inclined struts is 0.0025, while 0.0018 is the maximum strain that is logged at a horizontal strut.
6. The bottom tie recorded strain of the tested beams in case of concentrated forces are close to the yield value, while in case of uniformly distributed load, the bottom tie recorded strain is far from the yield value.
7. The first flexural cracks occur in positive bending moment in case of concentrated forces, while in case of uniformly distributed load, they occur in negative bending moment.
8. The convergence of the strains between top and bottom ties in case of uniformly distributed load is more than that in case of concentrated forces.

Notations	
A_b	Area of reinforcing bars, mm^2
A_h	Area of horizontal shear web reinforcement, mm^2
A_{sb}	Area of bottom main longitudinal tension reinforcement, mm^2
A_{st}	Area of top main longitudinal tension reinforcement, mm^2
b_w	Width of beam, mm
d	Effective depth of beam, distance from centroid of longitudinal tension reinforcement to the extreme compression fibre, mm
D_f	Displacement corresponding to the ultimate of deep beam, mm
$D_{diag.crack}$	Displacement corresponding to the 1st diagonal crack load, mm
$D_{n.crack}$	Displacement corresponding to the 1st negative flexural crack load, mm
$\Delta_{p.crack}$	Displacement corresponding to the 1st positive flexural crack load, mm
E_c	Modulus of elasticity of concrete, MPa
E_s	Modulus of elasticity of steel reinforcement, MPa
f'_c	Cylinder compressive strength of concrete, MPa
f_{ct}	Indirect tensile strength (splitting tensile strength), MPa
f_r	Modulus of rapture, MPa
f_y	Yield stress of main steel reinforcement, MPa
f_{yh}	Yield stress of horizontal web reinforcement, MPa
f_{yv}	Yield stress of vertical web reinforcement, MPa
h	Overall depth of deep beam, mm
j_d	Distance between the centres of the top and bottom nodes, mm
L	Total length of deep beam, mm
Lc	Length of span centre to centre, mm
Ln	Clear length of span, mm
L_w	Length of uniform load, mm
$P_{diag.crack}$	First diagonal cracking load, kN
$P_{n.crack}$	First negative flexural cracking load, kN

$P_{p.crack}$	First positive flexural cracking load, kN
P_{STM}	Theoretical load according to Appendix A, ACI 318M-14, Strut and Tie method, kN
P_f	Ultimate load failure, kN
W_f	Uniformly distributed load failure, kN/m
ε_{yield}	Strain at yield
ϑ	Inclination angle of the diagonal compressive stress and the failure plane with the beam longitudinal axis, degree
ρ	Flexural reinforcement ratio
$\emptyset$	Diameter of bar, mm
$\emptyset$main	Diameter of bar for main reinforcement, mm
$\emptyset$st	Diameter of bar for shear reinforcement, mm
a/d	Shear span to effective depth ratio
a/h	Shear span to overall depth ratio
ACI	American Concrete Institute
AISC-LRFD	American Institute of Steel Construction -load and resistance design specification
ASCE	American Society of Civil Engineers
ASTM	American Society for Testing and Materials
BT	Strain of bottom tie
c/c	Center to center, mm
CSA	Canadian Standard Association
ESC1	Longitudinal strain of external concrete strut
ESC2	Transverse strain of external concrete strut
ESS	Strain of external steel strut
HSC1	Longitudinal strain of horizontal concrete strut
HSC2	Transverse strain of horizontal concrete strut
HSS	Strain of horizontal steel strut
I.Q.S	Iraqi Standard Specification
ISC1	Longitudinal strain of internal concrete strut
ISC2	Transverse strain of internal concrete strut
ISS	Strain of external steel strut
Ln/h	Clear span to overall depth ratio
RC	Reinforced Concrete
STM	Strut and Tie Model
TT	Strain of top tie

REFERENCES

[1] Abdul-Razzaq, K. S. Effect of heating on simply supported reinforced concrete deep beams. *Diyala Journal of Engineering Sciences*, 8(2),2015,pp. 116-133.

[2] Abdul-Razzaq, K. S., Abed, A. H. and Ali, H. I. Parameters affecting load capacity of reinforced self-compacted concrete deep beams. *International Journal of Engineering*, 5(05), 2016, pp. 225-233.

[3] Abdul-Razzaq, K. S., Ali, H. I. and Abdul-Kareem, M. M. A New Strengthening Technique for Deep Beam Openings Using Steel Plates. *International Journal of Applied Engineering Research*, 12(24),2017, pp. 15935-15947.

[4] Abdul-Razzaq, K. S. and Jebur, S. F. Suggesting Alternatives for Reinforced Concrete Deep Beams by Reinforcing Struts and Ties. *MATEC Web of Conferences*, 120,2017.

[5] Abdul-Razzaq, K. S. and Farhood, M. A. Design and Behavior of Reinforced Concrete Pile Caps: A Literature Review. *International Journal of Engineering Research and science & Technology*, 6(4),2017.

[6] Abdul-Razzaq, K. S. and Jebur, S. F. Experimental Verification of Strut and Tie Method for Reinforced Concrete Deep Beams under Various Types of Loadings. *Journal of Engineering and Sustainable Development*, 21(6),2018, pp. 39-55.

[7] Abdul-Razzaq, K. S., Jebur, S. F. and Mohammed, A. H. Concrete and Steel Strengths Effect on Deep Beams with Reinforced Struts. *International Journal of Applied Engineering Research*, 13(1),2018, pp. 66-73.

[8] ACI Committee and American Concrete Institute, Building code requirements for structural concrete (ACI 318-14) and commentary, 2014.

[9] Merritt, F. S. and Ricketts, J. T. Building design and construction handbook. New York, NY, USA: McGraw-Hill, 2001.

[10] Wu, T. and Li, B. Experimental Verification of Continuous Deep Beams with Openings Designed Using Strut-and-Tie Modelling. *The IES Journal Part A: Civil & Structural Engineering*, 2(4), 2009, pp. 282–295.

[11] Abdul-Razzaq, K. S. and Jalil, A. M. Behavior of Reinforced Concrete Continuous Deep Beams-Literature Review. *The Second Conference of Post Graduate Researches (CPGR'2017) College of Engineering*, Al-Nahrain Univ., Baghdad, Iraq-4th Oct., 2017, pp.158-163.

[12] Abdul-Razzaq, K. S., Jebur, S. F. and Mohammed, A. H. Strut and Tie Modeling for RC Deep Beams Under Non-Central Loadings. *Civil Engineering Journal*, 4(5), 2018, 937-948.

[13] Jalil, A. M., Hamood, M. j., Abdul-Razzaq, K. S. and Mohammed, A. H. Applying Different Decentralized Loadings on RC Continuous Deep Beams using STM. *International Journal of Civil Engineering and Technology (IJCIET)*, 9 (11), 2018, pp. 2752-2769.

[14] Dawood, A. A., Kadhum, A. K. and Abdul-Razzaq, K. S. Strength of Reinforced Concrete Corbels – A Parametric Study. *International Journal of Civil Engineering and Technology (IJCIET)*, 9 (11), 2018, pp. 2274-2288.

[15] Abdul-Razzaq, K. S., Jalil, A. M. and Mohammed, A. H. Applying Various Types of Loading on Continuous Deep Beams Using Strut and Tie Modelling. *International Journal of Engineering & Technology (IJET)*, 7(4.2), 2018, pp. 251-258.

[16] ASTM A615/A615M-05, Standard Specification for Deformed and Plain Carbon-Steel Bars for Concrete Reinforcement, ASTM Committee A-1 on Steel, Stainless Steel, and Related Alloys, West Conshohocken, 2005, PA 19428-2959, United States, pp. 5.

[17] ASTM A496-02, Standard specification for steel wire, deformed, for concrete reinforcement, ASTM Committee A-1 on steel, stainless steel, and related alloys, West Conshohocken, 2002, PA 19428-2959, United States, pp. 5.